https://doi.org/10.5194/egusphere-2024-1820
Preprint. Discussion started: 3 July 2024

Toward more robust NPP projections in the North Atlantic Ocean

Stéphane Doléac[1], Marina Lévy[1], Roy El Hourany[2], and Laurent Bopp[3]

[1]Sorbonne Université, Laboratoire d'Océanographie et du Climat: Expérimentations et Analyses Numériques de l'Institut Pierre Simon Laplace (LOCEAN-IPSL), CNRS/IRD/MNHN, Paris
[2]Univ. Littoral Côte d'Opale, Univ. Lille, CNRS, IRD, UMR 8187, LOG, Laboratoire d'Océanologie et de Géosciences, F 62930 Wimereux, France
[3]LMD-IPSL, Ecole Normale Supérieure – Université PSL, CNRS, École Polytechnique, Sorbonne Université, Paris, France

Correspondence: Stéphane Doléac (stephane.doleac@locean.ipsl.fr)

Abstract.

Phytoplankton plays a crucial role in both climate regulation and marine biodiversity, yet it faces escalating threats due to climate change. Projecting the future changes in phytoplankton biomass and productivity under climate change requires the utilization of Earth System Models capable of resolving marine biogeochemistry, and exploits the averaged responses across an ensemble of models (within the Coupled Model Intercomparison Project Phase 6, CMIP6) as the most probable projection. However, in the North Atlantic, this straightforward method falls short in providing robust projections of phytoplankton net primary production (NPP) over the 21st century. This is because the processes controlling NPP strongly differ from one model to another, thus causing model divergence. A new inter-comparison approach was therefore developed and applied to 8 CMIP6 models exhibiting substantial divergence in their NPP projections in the North Atlantic. This approach is based on the identification of the mechanisms causing model divergence and the assessment of their reliability, in order to conduct an informed selection of the most reliable models. The basin was first divided into 3 bioregions tailored to the characteristics of each model using a novel method based on a clustering procedure. Two key mechanisms causing model divergence were then identified in the subtropical and subpolar regions (namely, diazotrophy and the presence of an ammonium pool, respectively). This allowed for an informed selection of models in each region, resulting in reduced uncertainty and a more pronounced decrease in total NPP in the subtropical North Atlantic and a stronger increase of small phytoplanton NPP in the subpolar North Atlantic. Our model selection strengthened carbon export and phytoplankton biomass decreases under climate change, but had no impact on zooplankton biomass. By leveraging the diversity of CMIP6 models, this innovative approach identifies the key mechanisms influencing NPP projections and provides valuable insights into the future trajectory of the Earth's climate system.

1 Introduction

The world's oceans are facing increasing pressures due to climate change, leading to significant alterations in their physical and biogeochemical conditions. Sea Surface Temperature (SST) has risen by an average of 0.88 °C between 1850-1900 and 2011-2020 (Fox-Kemper et al., 2021), pH has declined by 0.016 to 0.020 units per decade in the subtropical regions since the

https://doi.org/10.5194/egusphere-2024-1820
Preprint. Discussion started: 3 July 2024

1980s (Canadell et al., 2021) while upper-ocean stratification has increased by $5.5 \pm 1.0\%$ between 1960 and 2018 (Li et al., 2020). These changes pose a threat to the oceans' ability to provide essential environmental services that many people rely on, such as fisheries or carbon sequestration. Phytoplankton is key to many of these services and understanding how climate change will impact it is of primary importance, but still remains an open question.

The global distribution of phytoplankton is highly heterogeneous and is strongly influenced by ocean dynamics. The North Atlantic Ocean displays sharp contrasts, featuring a true "sea desert" in its subtropical section and one of the most productive regions on Earth in its subpolar part (Behrenfeld and Falkowski, 1997; Westberry et al., 2008). This high productivity is notably facilitated by a nutrient stream associated with the Atlantic Meridional Overturning Circulation (AMOC), which transports nutrients from equatorial and southern regions to the North Atlantic (Williams et al., 2006, 2011; Palter and Lozier, 2008), as well as by deep convection areas that bring large quantities of nutrients to the surface (Abot et al., 2023). This elevated productivity supports rich ecosystems and, combined with ocean dynamics, enables the North Atlantic Ocean to sequester large amounts of organic carbon through the biological carbon pump (Nowicki et al., 2022).

Climate change has both direct and indirect effects on phytoplankton net primary production (NPP). Directly, NPP increases with rising temperatures (Eppley, 1972; Sauterey et al., 2023). Indirectly, climate change impacts nutrient supply and light availability. Nutrient fluxes are influenced locally and regionally by increased vertical stratification, which reduces vertical supplies (Bopp et al., 2013), and globally by the projected decrease in the AMOC intensity (Whitt, 2019). Sea ice retreat reduces light limitation in polar region (Vancoppenolle et al., 2013), while zooplankton grazing is also affected by global warming (Laufkötter et al., 2015; Rohr et al., 2023). The impacts of these mechanisms vary regionally and affect differently the different phytoplankton groups, potentially causing shifts in community structures and total abundance (Kléparski et al., 2023; Benedetti et al., 2021).

Given this intricate complexity, projecting the precise impact of climate change on phytoplankton NPP poses significant challenges. Earth-system models (ESMs) from the Coupled Models Intercomparison Project (CMIP) include all of the above processes and thus offer a comprehensive approach to evaluating climate change impact on NPP. CMIP provides standardized experimental protocols (Eyring et al., 2016) based on shared socioeconomic pathways (O'Neill et al., 2014; O'Neill et al., 2016), enabling comparison of projections across models. Traditionally, all available models from the same CMIP phase are studied together and are used to assess a projection uncertainty around the multi-model mean (Bopp et al. (2013); Fu et al. (2016); Kwiatkowski et al. (2020); Tagliabue et al. (2021)). Each model is given the same weight and the multi-model mean is often considered as the best available projection, as it is assumed to be less impacted by the particular sets of parametrisations used in individual models. But, Kwiatkowski et al. (2020) have shown that in the case of NPP projections with models from the sixth phase of CMIP (CMIP6), there was a strong divergence in NPP projections between models at the global scale. This was confirmed in particular regions such as the Indian and Atlantic oceans by Tagliabue et al. (2021). Thus in terms of NPP, the multi-model mean contains little information and may not be considered as a reliable estimate of its future evolution. An approach different from the multi-model mean is therefore needed to assess how NPP will respond to climate change under a given projection scenario.

https://doi.org/10.5194/egusphere-2024-1820
Preprint. Discussion started: 3 July 2024

The strong divergence of NPP between models happens despite a strong coherence between them on the evolution of the physical and biogeochemical variables controlling NPP, such as SST, Mixed Layer Depth (MLD), NO3 concentrations (Kwiatkowski et al., 2020) or the AMOC (Weijer et al., 2020). This suggests that the observed discrepancy originates from differences in the representation and parametrization of marine biogeochemistry processes in the different models. Therefore, if it was possible to identify which processes controlled NPP projections in the different models, and to estimate their relevance in explaining NPP future evolution, it would then be possible to assess projections reliability and to make an informed selection of models to obtain more robust and precise NPP projections.

The objective of the following study is to apply this procedure to CMIP6 models over the North Atlantic Ocean, a highly productive region exhibiting strong future divergence between models (Tagliabue et al., 2021). Because we hypothesise that the response to climate change differs depending on the biogeochemical regime, we divided the North Atlantic into three bioregions (polar, subpolar, subtropical) using a clustering procedure and assessed each subregion individually. Finally, we discuss how our revised estimates of NPP projections may affect carbon export and plankton biomass, as key proxies for the biological carbon pump and marine ecosystems.

2 Methodology

2.1 CMIP6 models

All the CMIP6 models assessed in this study include an ocean biogeochemistry component. For both the historical period and the SSP5-8.5 scenario (O'Neill et al., 2016), a prerequisite for each model was to have a minimum of three ensemble members with available outputs for primary production and for the five clustering variables employed to construct bioregions (Chlorophyll-a surface concentrations, sea surface temperature (SST), mixed layer depth (MLD), sea ice concentration, and nitrate surface concentrations). Out of the 16 models with primary production projections under the SSP5-8.5 scenario, only 8 fulfil these criteria. Among the 8 excluded models, 6 have only one member, and the remaining two (CNRM-ESM2-1 and MIROC-ES2L) lack one clustering variable for several or all members. Details about the characteristics of the remaining 8 models can be found in table 1.

Ensemble means for each model were computed to eliminate a maximum amount of natural variability, allowing us to focus on the impact of anthropogenic climate change. Trends were derived by averaging ensemble mean outputs over 20-year periods every five years from 1950-1970 to 2080-2100. These trends were calculated over the region between 10-80°N and 270-360°E, referred to as "the North Atlantic Ocean" in the subsequent analysis. The period 1950-1970 was taken as the reference and all projections were expressed as the evolution between this reference period and 2080-2100.

The complexity of ESM marine biogeochemistry components varies significantly from one model to another. Among the 8 models selected, the simplest model only includes one nutrient and one phytoplankton class (Zahariev et al., 2008) whereas the most model features 5 nutrients and three phytoplankton classes (Moore et al. (2001) ; see Kearney et al. (2021) for a summary of the biogeochemistry components of CMIP6 models). Due to these differences, each model is studied individually to comprehensively grasp the mechanisms controlling NPP projections.

https://doi.org/10.5194/egusphere-2024-1820
Preprint. Discussion started: 3 July 2024

Three phytoplankton groups were considered in this study : diatoms, diatozotrophs and small phytoplankton. The last category encompasses classes labelled as nanophytoplankton, picophytoplankton and bulk phytoplankton when sensitivity to silicate is absent. In MPI-ESM1-2-LR, the bulk phytoplankton class is grouped with diatoms due to its reliance on $SiO2$ (Ilyina et al., 2013), whereas the large phytoplankton class in CanESM5-CanOE is distinguished from diatoms due to the absence of silicate in the model (Christian et al., 2022). Furthermore, CMIP6 models can be categorized into three groups based on their representation of diazotrophy:

- Models without any diazotrophy: ACCESS-ESM1-5 and UKESM1-0-LL.
- Models with an explicit group of diazotrophs: CESM2, CESM2-WACCM, and MPI-ESM1-2-LR. In these models, diazotroph growth rate is not constrained by nitrogen; they can utilize atmospheric $N2$ but depend on $PO4$ and Fe availability (Moore et al. (2001) for CESM2 and CESM2-WACCM; Paulsen et al. (2017) for MPI-ESM1-2-LR).
- Models with an implicit representation of diazotrophs: IPSL-CM6A-LR, CanESM5, CanESM5-CanOE. $N2$ fixation is parametrized, and its interaction with other nutrients varies based on this parametrization.

2.2 Construction of bioregions

The processes governing changes in NPP vary across different regions, necessitating a regional approach. Bioregions are the most suitable framework for conducting such a study because each bioregion corresponds to a specific production regime. However, their boundaries align with physical phenomena such as oceanic currents and sea ice, the precise localization of which varies among models. Consequently, fixed bioregions like those established by Longhurst (2007) and used in Tagliabue et al. (2021) have limitations for inter-comparison studies.

To address this limitation, a novel approach was developed to establish bioregions tailored to the characteristics of each model. They were constructed using the SOM+HAC clustering procedure (defined in the following section), a robust method for extracting temporal and spatial patterns from large datasets. This procedure was first applied to the observed mean seasonal cycles over the recent historical period of five clustering variables, chosen for their relevance in explaining NPP long term evolution and their availability in CMIP6 models outputs. The bioregions obtained were then replicated in each model. By employing this method, we ensured that each bioregion corresponded to a similar production regime across all models.

2.2.1 The SOM+HAC procedure

The Self-Organizing Map (SOM) algorithm (Kohonen, 2013) is widely used for pattern identification and clustering analysis for large multi-variate datasets. In environmental sciences, it has been used to study precipitation patterns (Derouiche et al., 2022; Dilmi et al., 2017), monsoon weather regimes (Guèye et al., 2011)), phytoplankton biomes (El Hourany et al., 2021; Hofmann Elizondo et al., 2021), the oceanic circulation (Jouini et al., 2016), aerosol concentrations (Yahi et al., 2013) or to identify biophysical regions in the Beaufort sea (Hilborn and Devred, 2022). Similar to classical vector quantization procedures, such as K-mean clustering, the SOM algorithm condensates the information contained in a multi-variate dataset into an

https://doi.org/10.5194/egusphere-2024-1820
Preprint. Discussion started: 3 July 2024

optimal number of "neurons", each associated to a vector characterizing a subset of the initial dataset. However, unlike K-mean clustering, the neurons in the SOM algorithm are not independent. They are distributed over a 2D map with a topological constraint such that close neurons on the map are similar. Practically, this constraint means that, during the learning phase, neurons are not updated alone but as batches of close neurons, thus allowing the propagation of local updates to the global neuron map. This topological constraint allows the preservation of the topological properties of the initial dataset. An advantage of the SOM algorithm over K-mean clustering procedures is that it is robust to missing data (Vatanen et al., 2015), making it particularly interesting in the regions seasonally covered by sea ice.

When handling environmental data, the specific quantity of classes or neurons isn't predetermined. In cases where the SOM is employed for vector quantization, a large number of neurons are utilised, each assigned to a geographic sub-region. To determine major patterns among these neurons, a Hierarchical Agglomerative Clustering (HAC) is employed on them, while preserving the topological constraints. This procedure is denoted SOM+HAC hereafter. The HAC produces a dendrogram offering various suggestions for estimating the number of classes. A balance is struck between the number of classes that can be logically explained and the number required to encompass the data's embedded information. This approach has demonstrated success in numerous studies (Farikou et al., 2015; Jouini et al., 2016; El Hourany et al., 2021; Baaklini et al., 2022).

2.2.2 The datasets used to build bioregions

To ensure that the bioregions obtained in each model were similar, they were first constructed from the observations before being reproduced in the models (see the following subsection). Here, we describe the datasets of observations used to build these bioregions.

Surface chlorophyll-a concentrations were extracted from E.U. Copernicus Marine Service Global Ocean Colour product (https://doi.org/10.48670/moi-00281). It provides daily outputs of chlorophyll concentration, estimated from satellite data, over the global ocean between September 1997 and the present. Data from the period 2000-2020 were used.

Sea Surface Temperature and Mixed Layer Depth data were extracted from the Multi Observation Global Ocean 3D product from Copernicus Marine service (data.marine.copernicus.eu). It provides weekly and monthly values of 6 variables, among which SST and MLD, over the global ocean between 1993 and 2023, built from both in-situ and satellite observations. Again, data from the period 2000-2020 were used.

NO3 concentrations were extracted from the World Ocean Atlas 2018 database (Garcia et al., 2018) while sea ice concentration data came from the EUMETSAT OSI SAF SSMIS product (cds.climate.copernicus.eu) and covered the period 1998-2015.

2.2.3 Application of the clustering procedure

The SOM+HAC was first applied to the historical mean seasonal cycles of five clustering variables (surface chlorophyll concentrations, surface nitrate concentrations, mixed layer depth, sea ice concentration, and sea surface temperature) computed from the datasets previously described. They were regridded to 1x1° regular grids, concatenated and the coastal areas were removed. The North Atlantic Ocean was thus represented by 3335 grid points, each associated to a vector of dimension 60, corresponding to the 5 successive climatological seasonal cycles. To ensure equal weighting of all variables in the clustering

https://doi.org/10.5194/egusphere-2024-1820
Preprint. Discussion started: 3 July 2024

process, the dataset was normalized beforehand. Several normalization methods, such as those outlined in Derouiche et al. (2022); Dilmi et al. (2017); Hilborn and Devred (2022) can be employed. It was decided to normalize each seasonal cycle by dividing it by the absolute maximum value reached over the entire period and region. This normalization method has the advantage of preserving the dataset structure while ensuring all values fall within the range of -1 and 1. The selection of clustering variables resulted from a compromise between their relevance in explaining primary production variability in the North Atlantic Ocean and their availability in CMIP6 model outputs. For instance, silicate concentration was excluded, despite its acknowledged impact on primary production in the subpolar gyre (Hátún et al., 2017; Sieracki et al., 1993), as only 5 out of 8 models provided the output.

The neurons obtained from the observations were then used to replicate similar bioregions in the CMIP6 models. In each model, a matrix akin to that of the observations was reproduced with the average seasonal cycles over the period 2000-2020, using the same normalization method and constants. Each grid point in each model was subsequently assigned to its nearest neuron based on Euclidean distance and to the cluster associated with that neuron, thereby reproducing the bioregions in each model. This assignment was carried out regardless of the distance between the grid point and the neuron. Consequently, the regions obtained were the closest to those built from the observations but could be rather different from them.

3 Results

3.1 Global projections

Primary production projections over the whole North Atlantic Ocean with CMIP6 models exhibit a large spread (see figure 1-A). Among the eight models, five (UKESM1-0-LL, CESM2, CESM2-WACCM, MPI-ESM1-2-LR and CanESM5) project a strong decrease of net primary production (from -33.6 to -11.4 $\mathrm{g.m^{-2}.yr^{-1}}$ in 2080-2100 with respect to 1950-1970), while the remaining three (CanESM5-CanOE, IPSL-CM6A-LR, ACCESS-ESM1-5) project an increase (from +8.0 to +17.0 $\mathrm{g.m^{-2}.yr^{-1}}$). On average, CMIP6 models project an NPP decrease of -10.4 $\mathrm{g.m^{-2}.yr^{-1}}$. This range is similar to the one obtained with the first member of the 16 models used in Tagliabue et al. (2021). Therefore, the selected subset of eight models is considered representative of the broader ensemble of CMIP6 models.

There is confidence in the sign of NPP projections in the north-eastern section of the subtropical gyre and along Greenland eastern coast only (fig. 1-D). Confidence is defined here following Kwiatkowski et al. (2020) with at least 80 % of the projections have the same sign. Models disagree on the sign of the future evolution of NPP in most of the subpolar gyre and in the southern subtropical gyre. This lack of confidence happens despite a strong coherence between models on the evolution of MLD and surface nitrate concentrations, particularly in the subpolar North Atlantic Ocean (fig. 1-E,F). On average over the region, all models project a decrease of MLD and NO3 concentrations, with a multi-model mean decrease of respectively -22.1 m and -1.3 $\mathrm{mmol.m^{-3}}$.

https://doi.org/10.5194/egusphere-2024-1820
Preprint. Discussion started: 3 July 2024

3.2 Construction of the bioregions

The SOM+HAC procedure identified an optimal number of four bioregions in the observations: one subtropical region, one polar region, and two subpolar regions. The subtropical bioregion, the largest at 20.8 million km^2, exhibits an oligotrophic regime characterized by very low nitrate and chlorophyll-a concentrations (maximum annual values of respectively 0.87 $\mathrm{mmol.m^{-3}}$ and 0.16 $\mathrm{mg.m^{-3}}$). It is situated over the subtropical gyre and the Caribbean Sea, bordered by the North Atlantic Current to the north. The polar region, the smallest at 1.0 million km^2, stands out due to the extensive presence of sea ice during winter and is further divided into two subregions: the Baffin Sea and the Eastern Greenland Sea. The two subpolar regions, with surfaces of 3.3 and 4.8 million km^2, respectively correspond to the intergyre region with the northern part of the Labrador Sea and the northern subpolar gyre with the Norwegian Sea. The latter region exhibits a deeper winter mixed layer, higher nitrate surface concentrations, and a delayed bloom compared to the former. However, the two regions do not significantly differ in terms of annual maximum chlorophyll-a concentrations (0.76 $\mathrm{mg.m^{-3}}$ in August for the former and 0.80 $\mathrm{mg.m^{-3}}$ in September for the latter).

Qualitatively, models reproduce fairly well the historical bioregions obtained from observations, both in terms of localization and physical boundaries, and despite variations in surfaces (fig. 2). The subtropical region's surface ranges from 19.1 million km^2 in MPI-ESM1-2-LR to 24.1 million km^2 in CanESM5, while the polar region's surface varies from 0.9 million km^2 in MPI-ESM1-2-LR to 2.0 million km^2 in CanESM5. The overall subpolar region is relatively consistent across different models, but the relative importance of the subregions varies significantly from one model to another. It was decided to merge the subpolar subregions into one large subpolar region, supported by strong inter-model correlations between the projections of NPP in the two regions (r = 0.91; p = 0.002), indicating a similar dominant mechanism. The three resulting bioregions are presented for the observations and each models on figure 2. Each of these bioregions will now be studied successively to determine the mechanisms controlling NPP projections.

3.3 Regional analysis

3.3.1 Subtropical region

NPP projections strongly diverge in the subtropical region, with three models projecting an increase (up to +19.5 $\mathrm{g.m^{-2}.yr^{-1}}$ in 2080-2100 with respect to the 1950-1970 mean), while the remaining five project a decrease (down to -33.4 $\mathrm{g.m^{-2}.yr^{-1}}$) (figure 3). These divergent groups align with those observed for the entire North Atlantic Ocean (figure 1-A), suggesting that the subtropical region predominantly influences the basin-scale divergence of projections.

This substantial discrepancy occurs despite coherent evolutions across models for other crucial physical and biogeochemical variables (fig. 3). Notably, sea surface temperature (SST) increases in all models (ranging from +2.7 °C in MPI-ESM1-2-LR to 5.3 °C in CanESM5), while surface $\mathrm{NO3}$ concentrations and surface $\mathrm{PO4}$ concentrations decrease ($\mathrm{NO3}$ concentrations from -0.19 to -0.69 $\mathrm{mmol.m^{-3}}$; $\mathrm{PO4}$ concentrations from -0.01 to -0.13 $\mathrm{mmol.m^{-3}}$). Mixed layer depth and carbon export at 100m depth both decrease in all models but one (respectively ACCESS-ESM1-5 and IPSL-CM6A-LR), in which they increase after a period of decrease.

https://doi.org/10.5194/egusphere-2024-1820
Preprint. Discussion started: 3 July 2024

Diatom NPP decreases in all models and therefore does not explain total NPP discrepancy. It is almost perfectly correlated with the evolution of surface PO4 concentrations in all models ($r \geq 0.99$, $p \ll 0.01$; fig. 4). The inter-model spread thus arises from differences in sensitivity to a similar mechanism. Conversely, small phytoplankton's NPP exhibits a strong discrepancy, thus explaining that of total NPP. The only variable able to cause this divergence is N2 fixation, for which a clear separation appears between models with an implicit representation of diazotrophs, which project a strong increase of N2 fixation, and those with an explicit representation, who project a decrease in diazotrophs' NPP (fig. 3). As detailed in the Methodology section, CMIP6 models can be categorized into three groups according to their representation of N2 fixation. We will now examine each of these groups individually.

The two models with no diazotrophy project different primary production evolutions (ACCESS-ESM1-5 projects an increase of 10.0 $\mathrm{g.m^{-2}.yr^{-1}}$, while UKESM1-0-LL projects a decrease of -33.4 $\mathrm{g.m^{-2}.yr^{-1}}$). In UKESM1-0-LL, the production of both nanophytoplankton and diatoms decreases (figure 3). This discrepancy is mainly attributed to variations in annual maximum surface nitrate concentrations (respectively 1.0 and 0.3 $\mathrm{mmol.m^{-3}}$ on average in 2000-2020 ; the observed value is 0.4 $\mathrm{mmol.m^{-3}}$). In UKESM1-0-LL, nitrates are strongly limitant, and their declining trend (see figure 3-G) leads to a decreased primary production for all phytoplankton groups. In ACCESS-ESM1-5, nitrates are not a strong limitation on average across the entire subtropical region, allowing primary production to increase with rising SST.

The three models with an explicit representation of diazotrophs all project a decrease in both primary production and N2 fixation. This decrease affects both diazotrophs and diatoms in these models, while small phytoplankton primary production in CESM2 and CESM2-WACCM initially increases before decreasing (fig. 3). This coherence across phytoplankton groups suggests that the mechanism influencing primary production evolution could affect all of them, ruling out nitrates as a potential candidate, as they do not impact diazotrophs. The only variable capable of explaining these evolutions is PO4 concentrations, influencing all phytoplankton groups, consistently decreasing in all three models and known to limit N2 fixation in the region in CESM models (Wang et al., 2019). Additionally, in CESM2 and CESM2-WACCM, small phytoplankton has a lower PO4 half-saturation constant than diazotrophs and diatoms (respectively 0.00025, 0.0005 and 0.00125 $\mathrm{mmol.m^{-3}}$ (Moore et al., 2001)), enabling them to thrive in environments with low PO4 concentrations. This explains the initial increase in their primary production before declining when PO4 concentrations become too low. Consequently, in models with an explicit representation of diazotrophs, decreasing PO4 concentrations leads to a reduction in overall primary production, encompassing diazotrophs, subsequently causing a decrease in N2 fixation.

In IPSL-CM6A-LR, the absence of effective control of PO4 concentrations over N2 fixation was identified as responsible for the substantial increase in diazotrophy and primary production in subtropical oceans (Bopp et al., 2022). The increase in N2 fixation fills the NH4 pool (Aumont et al., 2015), which can then serve as an alternative source of nitrogen for small phytoplankton, and thus lead to its increase despite a decrease in NO3 concentrations. CanESM5-CanOE also has an ammonium pool directly filled by N2 fixation and no PO4 pool. Therefore, like in IPSL-CM6A-LR, the increase of N2 fixation results in an increase of small phytoplankton NPP. However, unlike in IPSL-CM6A-LR, this increase also happens for large phytoplankton because PO4 can not exert its control. Finally, in CanESM5, there is a unique nitrogen pool assembling both ammonium

https://doi.org/10.5194/egusphere-2024-1820
Preprint. Discussion started: 3 July 2024

and nitrates. The increase in N2 fixation fails to offset its decrease from other mechanisms, thus leading to a decrease in NPP (fig. 3).

The interactions between N2 fixation, phosphates and small phytoplankton therefore appear to be a strong diverging factor between models, with the potential to partially decouple total NPP from NO3 concentrations. The models with the most realistic representations of diazotrophy (CESM2, CESM2-WACCM and MPI-ESM1-2-LR) all project a decrease of NPP because of the declining PO4 concentrations. The strong increases observed in some models are caused by either too high nitrate concentrations when no diazotrophy is represented, or by its unchecked influence by PO4 concentrations, making such scenarios unlikely.

3.3.2 Subpolar region

NPP projections also significantly diverge in the subpolar region (fig. 5-A). Three models (CESM2, CESM2-WACCM, and UKESM1-0-LL) project a substantial decrease (respectively -54.3, -53.7 and -44.7 $\mathrm{g.m^{-2}.yr^{-1}}$ in 2080-2100 with respect to 1950-1970), while three others (IPSL-CM6A-LR, CanESM5-CanOE, and ACCESS-ESM1-5) project a modest increase (respectively +5.4, +6.6 and +3.8 $\mathrm{g.m^{-2}.yr^{-1}}$). The remaining two models project an intermediate decline (-12.7 $\mathrm{g.m^{-2}.yr^{-1}}$ in MPI-ESM1-2-LR and -10.0 $\mathrm{g.m^{-2}.yr^{-1}}$ in CanESM5). This disparity persists despite consistent trends across models for other physical and biogeochemical variables, such as SST, MLD, AMOC intensity, carbon export, NO3 and PO4 surface concentrations (fig. 5). However, the breakdown of NPP projections into the different phytoplankton groups highlights that it is predominantly small phytoplankton that drives their divergence (fig. 5). Diatom NPP consistently decreases in all models.

Remarkably strong and statistically significant correlations ($r > 0.96$, $p \ll 0.01$) were identified in all models between diatom NPP projections and surface maximum annual NO3 concentrations (fig. 4). Like in the subtropical bioregion, this suggests that the inter-model spread of diatom NPP projections comes from differences in sensitivity to a similar mechanism.

Five models out of seven project an increase in small phytoplankton's NPP, despite a decrease of NO3 and PO4 concentrations coherent across models (fig. 5). Of these five models, four (IPSL-CM6A-LR, CanESM5-CanOE, CESM2, and CESM2-WACCM) incorporate an ammonium pool. In IPSL-CM6A-LR, CESM2, and CESM2-WACCM, where the distinct contributions of NO3 and NH4 to primary production can be discerned, it is primarily NH4 that sustains it. This suggests a similar situation in CanESM5-CanOE, where the increase in small phytoplankton's primary production is likely caused by the rising temperatures and shallowing of MLD and sustained by NH4. However, these increases are only able to compensate for diatoms decreases in IPSL-CM6A-LR, thus explaining the sign of the evolution of total NPP. The increased NPP of small phytoplankton in ACCESS-ESM1-5, where there is no NH4 pool, was attributed to the absence of nitrate limitation (minimum annual concentration averaging 1.5 $\mathrm{mmol.m^{-3}}$ over 2080-2100 despite a consistent decrease throughout the 21st century). The elevation in SST and the reduction of light limitation due to the shallowing of MLD can consequently enhance NPP. Conversely, in UKESM1-0-LL and CanESM5, nitrates exert strong limitations (minimum annual concentration averaging 0.04 and 0.003 $\mathrm{mmol.m^{-3}}$, respectively, over 2080-2100), and their depletion leads to a reduction in NPP.

The strong increase of small phytoplankton's NPP observed in some CMIP6 models is therefore made possible by the presence of an ammonium pool, which stands up as an alternative source of nitrogen and sustains NPP. NH4 is only present in

https://doi.org/10.5194/egusphere-2024-1820
Preprint. Discussion started: 3 July 2024

small concentration, but is quickly regenerated, and is therefore preferentially used by small phytoplankton rather than diatoms. It explains why diatoms can not benefit from it and decrease with macro-nutrient concentrations.

3.3.3 Polar region

Primary production increases in all models in the polar region, ranging from +6.2 to +25.5 $\mathrm{g.m^{-2}.yr^{-1}}$ in 2080-2100 with respect to 1950-1970 (fig. 6). These increase are mainly caused by sea ice retreat (on average, 36.4 % of the initial polar regions were still covered in sea ice in winters in 2080-2100), which leaves space for phytoplankton's growth, and thus leads to an increase in NPP. However, like in the rest of the subpolar regions, $\mathrm{NO3}$ and $\mathrm{PO4}$ surface concentrations decrease in all models (fig. 6).

This increase in total NPP is observed in all models for small phytoplankton, but not for diatoms, for which three models (CESM2, CESM2-WACCM and UKESM1-0-LL) project a decrease of their primary production after an initial increase (fig. 6). These three models are the most sensitive to a decrease in $\mathrm{NO3}$ concentrations, as they have the highest half-saturation constants of the 6 models (2.5 $\mathrm{mmol.m^{-3}}$ for CESM2 and CESM2-WACCM Moore et al. (2001)); 0.75 $\mathrm{mmol.m^{-3}}$ for UKESM1-0-LL Yool et al. (2013)). Moreover, they all reach very low annual minimum $\mathrm{NO3}$ concentrations (respectively 0.02, 0.02 and 0.19 $\mathrm{mmol.m^{-3}}$ in 2080-2100), indicating a termination of the bloom by nitrates. Therefore, in these three models, after a first period in which the retreat of sea ice leads to an increase in primary production through the reduction of light limitation, nitrates become the main controlling factor of primary production, which leads to its decrease. In IPSL-CM6A-LR, nitrate concentrations are even lower than in the previous models (annual minimum of 0.01 $\mathrm{mmol.m^{-3}}$ in 2080-2100), but diatoms are less sensible to low nitrate concentrations (half-saturation constant of 0.39 $\mathrm{mmol.m^{-3}}$ (Aumont et al., 2015)) and their primary production can keep increasing under the reduction of light limitation. In MPI-ESM1-2-LR, nitrate concentrations are high throughout the XXI^{st} century (annual minimum concentration of 1.18 $\mathrm{mmol.m^{-3}}$ in 2080-2100 despite a consistent decrease throughout the century), and never become limitant. Diatom primary production can therefore freely increase with sea ice retreat.

To summarize, climate change leads to an increase of small phytoplankton NPP in all CMIP6 models because of sea ice retreat. The fate of diatoms is the result of a compromise between their sensitivities to light, to nitrates and the evolutions of $\mathrm{NO3}$ concentrations and sea ice, as was already the case in CMIP5 (Vancoppenolle et al., 2013). However, only a small portion of the Arctic was included in this study, and the results found can not be expanded to the total Arctic ocean.

3.4 Toward more robust NPP projections

The model representation of small phytoplankton emerged as the main cause of divergence in NPP projections between models in the subtropical and subpolar North Atlantic Ocean. In the subtropical basin, differing representations of diazotrophy explain model disparities. When not adequately regulated by nutrients like $\mathrm{PO4}$, it has the potential to significantly boost small phytoplankton's NPP while other nutrient concentrations decline. Only the 3 models explicitly representing diazotrophs represent these controls and project a decrease in NPP. The three models with an implicit representation of diazotrophs, and no effective control from $\mathrm{PO4}$, are therefore not reliable for studying the evolution of small phytoplankton's NPP in the region. Among the

https://doi.org/10.5194/egusphere-2024-1820
Preprint. Discussion started: 3 July 2024

models without diazotrophy, ACCESS-ESM1-5 emerged as overly rich in nutrients on average across the subtropical region, making it unreliable for projecting average NPP evolution. Thus, only four out of the eight models appeared dependable for projecting small phytoplankton's NPP evolution in the region (MPI-ESM1-2-LR, CESM2, CESM2-WACCM and UKESM1-0-LL). They project an average decrease of -4.8 $\mathrm{g.m^{-2}.yr^{-1}}$ (from -26.0 to +6.4 $\mathrm{g.m^{-2}.yr^{-1}}$), against -2.2 $\mathrm{g.m^{-2}.yr^{-1}}$ (from -26.0 to +20.4 $\mathrm{g.m^{-2}.yr^{-1}}$) with all models (fig. 7-C). This selection also leads to a strengthening of diatoms NPP projected decrease (fig. 7-B), thus resulting in a total NPP decrease of -24.9 [-33.4 - -20.3] $\mathrm{g.m^{-2}.yr^{-1}}$ (against -8.2 [-33.4 - 19.5] $\mathrm{g.m^{-2}.yr^{-1}}$; fig. 7-A).

In the subpolar region, $\mathrm{NH4}$ appeared to be able to sustain small phytoplankton's NPP in the models where it is present (IPSL-CM6A-LR, CanESM5-CanOE, CESM2, and CESM2-WACCM). If we hypothesize that ammonium will indeed play such a role in reality, models without an ammonium pool then tend to overestimate the impact of decreasing $\mathrm{NO3}$ concentrations on small phytoplankton. We can therefore set them aside and obtain narrowed estimates of small phytoplankton's NPP projections: +21.4 $\mathrm{g.m^{-2}.yr^{-1}}$ (from +6.4 to +35.0 $\mathrm{g.m^{-2}.yr^{-1}}$) instead of 7.3 $\mathrm{g.m^{-2}.yr^{-1}}$ (from -28.2 to +35.0 $\mathrm{g.m^{-2}.yr^{-1}}$) with all models (fig. 7-F). However, such an hypothesis would have no impact on total NPP because it would not affect diatoms (fig. 7-E) and the extreme models would be kept in the subset : -24.0 $\mathrm{g.m^{-2}.yr^{-1}}$ (from -54.3 to +6.6 $\mathrm{g.m^{-2}.yr^{-1}}$) instead of -20.0 $\mathrm{g.m^{-2}.yr^{-1}}$ (from -54.3 to +6.6 $\mathrm{g.m^{-2}.yr^{-1}}$) with all models (fig. 7-D).

The contrast in the impact of model selection on diatoms between the subtropical and subpolar regions suggests that the mechanisms driving divergence in small phytoplankton also influence diatoms in the former but not the latter. In both regions, diatoms are predominantly governed by the same mechanism: a reduction in macro-nutrient concentrations results in a decrease in diatom NPP (fig. 4). However, the magnitude of this reduction is notably greater in the subpolar region compared to the subtropical region. Consequently, the influence of $\mathrm{NH4}$ on diatoms in the subpolar region is negligible, whereas that of diazotrophy in the subtropical region is not. Therefore, selecting models based on the processes governing small phytoplankton NPP projections leads to narrowed projections for diatoms and total NPP in the subtropical region but not in the subpolar one.

In the polar region, no discriminating mechanism was identified and it was not possible to narrow projections using the same method.

3.5 Impact on carbon export and plankton biomass

NPP is closely linked with carbon export and plankton biomass, which are crucial variables for comprehending the future trajectory of the biological carbon pump and the effects of climate change on marine ecosystems. Consequently, the process-based selection of NPP models made previously can be used to estimate new projections of these other two variables.

Projections for carbon export across the global North Atlantic Ocean reveal significant disparities, ranging from -8.7 to +0.3 $\mathrm{g.m^{-2}.yr^{-1}}$, with an average decrease of -3.9 $\mathrm{g.m^{-2}.yr^{-1}}$. However, there is less uncertainty regarding the direction of its future changes compared to NPP projections (table 2). While some models anticipate a slight increase in the subtropical region, all models project a decline in carbon export in the subpolar region. The model selection allows for a reduction of projection uncertainties in the subtropical region, resulting in a larger average decrease (-5.7 $\mathrm{g.m^{-2}.yr^{-1}}$ on average compared to -3.5 $\mathrm{g.m^{-2}.yr^{-1}}$ with all models). In the subpolar region, it does not reduce projection uncertainties, but strengthen the average

https://doi.org/10.5194/egusphere-2024-1820
Preprint. Discussion started: 3 July 2024

decrease (table 2). The slight global increase of carbon export projected by some models is therefore explained by the strong increase of NPP they project in the subtropical region, and is therefore unlikely to happen. The NPP process-based selection of models thus strengthen carbon export decrease at the end of the XXIst century in the North Atlantic Ocean.

Phytoplankton biomass projections also exhibit a strong discrepancy, similar to that of NPP for the global North Atlantic Ocean and for the subtropical region (table 2). However, the future evolution of phytoplankton biomass in the subpolar region is less uncertain compared to NPP, despite considerable model divergence (table 2). The selection of models leads to a significant reduction of projection uncertainties in the subtropical region, where a new inter-model agreement on a future decrease of phytoplankton biomass emerges. The strong increases projected by some models are therefore caused by their inadequate representation of diazotrophy in the subtropical region, making such projections improbable.

All models agree on a decrease of zooplankton biomass across the global North Atlantic Ocean and in the two individual regions (table 2). Both selections only slightly narrow projections in the two regions. This limited impact is due to the varying representations of zooplankton in CMIP6 models (Rohr et al., 2023), leading to a relative inter-model decoupling of phytoplankton and zooplankton. An analysis similar to the one conducted here should therefore be done to fully understand zooplankton projections in CMIP6 models.

4 Discussion

4.1 Model democracy and emergent constraints

NPP projections in the North Atlantic Ocean emerged as a case where the traditional approach of model inter-comparison studies through "model democracy" may not be adapted. This approach assumes that all ESMs are equally relevant and reliable for projecting future climate evolution (Knutti, 2010), whereas we showed here that some models, due to their representation or lack thereof of certain processes, are not dependable for projecting NPP in the region. A democratic multi-model mean computed with equal weights attributed to all models, as is done in Kwiatkowski et al. (2020) and Tagliabue et al. (2021), would therefore not be the optimal estimate of the future evolution of NPP.

However, we did not entirely set aside the "model democracy" approach, because it was applied to model subsets in both regions. This application is questionable because it assumes independence among selected models, which is often not the case (Eyring et al., 2019). Some CMIP6 models are essentially variations of a similar base model (e.g., CESM2 and CESM2-WACCM) and share components and parametrizations (Masson and Knutti, 2011; Bishop and Abramowitz, 2013; Alexander and Easterbrook, 2015). This lack of independence results in systematic biases within multi-model mean when "model democracy" is adopted. To address this issue, various studies have attempted to assign different weights to models based on their independence and ability to reproduce historical observations (Sanderson et al., 2015, 2017). While such efforts have sometimes improved agreement between multi-model means and observations (Räisänen et al., 2010; Knutti et al., 2017), the question of the validity of weighting methods for future projections remains unresolved. For example, in the context of NPP projections in the subtropical North Atlantic Ocean, discrepancies in diazotrophy between models with effective $PO4$ control and those without only arise around the year 2020 (fig. 3). Consequently, weighting based solely on observations would likely

https://doi.org/10.5194/egusphere-2024-1820
Preprint. Discussion started: 3 July 2024

overlook this divergence. Thus, process-based model selections, such as the one conducted here, and weighting methods are complementary techniques that should ideally be used together to maximize their respective advantages.

Moreover, our approach failed at improving total NPP projections in the subpolar North Atlantic Ocean, because we were not able to constrain diatoms. The discrepancy of diatom NPP projections arise from differences in sensitivity to a similar mechanism (fig. 4), which prevents a process-based approach. However, it might set a good framework for an Emergent constraint approach, which consists in exploiting an inter-model correlation between an observable variable and the response of another variable to climate change to constrain projections (Eyring et al., 2019; Sanderson et al., 2021). Emergent constrains have successfully been used to constrain projections of climate sensitivity (Cox et al., 2018), sea-ice extent (Qu and Hall, 2014), extreme precipitation events (O'Gorman, 2012), or NPP in the tropical ocean (Kwiatkowski et al., 2017). But, the reliability of emergent constraint outcomes is often hindered by the presence of systematic biases in large-ensembles, stemming from model interdependence (Sanderson et al., 2021). Nevertheless, it is sometimes possible to enhance this reliability with the identification of a robust mechanism explaining the correlation used. Emergent constraints and process-based approaches are therefore complementary, particularly when competing mechanisms coexist. The case of NPP projections in the subpolar North Atlantic Ocean thus seems to be an ideal situation for combining a process-based method applied to small phytoplankton, carried out in this study, with an emergent constraint approach applied to the differing sensitivities of diatom NPP to nitrate concentrations. This will be the objective of a future study.

4.2 Estimation of climate change impacts on high trophic levels

CMIP model output serves as data inputs for the Inter-Sectoral Impact Model Intercomparison Project (ISIMIP), an exercise aimed at examining the effects of climate change on human societies and ecosystems (Frieler (2024); https://protocol.isimip.org/). In the context of studying fisheries and marine ecosystems, CMIP models are used as inputs for marine ecosystem models. Depending on the model employed, the connecting variable between plankton and higher trophic levels could be either NPP or the biomass of phytoplankton and zooplankton (Tittensor et al., 2021). However, only a limited selection of CMIP models are incorporated into these studies. For the third phase of ISIMIP, specifically, only four CMIP6 models were chosen for marine ecosystem studies: GFDL-ESM4, UKESM1-0-LL, MPI-ESM1-2-HR, and IPSL-CM6A-LR. The biases exhibited by these models in projecting NPP and plankton biomass consequently influence the marine ecosystem models that employ them to investigate climate change impacts.

We demonstrated that IPSL-CM6A-LR lacks reliability in projecting NPP in the subtropical region due to its failure to represent $PO4$ control over $N2$ fixation. Conversely, UKESM1-0-LL lacks an $NH4$ pool, likely resulting in an overestimation of NPP decrease in the subpolar region. These model deficiencies in projecting NPP directly affect phytoplankton biomass, and similar issues may arise for zooplankton biomass due to their disparate representations across CMIP6 models (Rohr et al., 2023). Such biases could significantly impact ISIMIP outcomes, which are subsequently used by policymakers to develop adaptation measures to climate change. Hence, it is imperative to identify these biases, assess the reliability of CMIP models in projecting variables used in ISIMIP studies, and estimate the repercussions of CMIP biases on ISIMIP results.

https://doi.org/10.5194/egusphere-2024-1820
Preprint. Discussion started: 3 July 2024

4.3 Perspectives on the future evolution of the biological carbon pump

Carbon export caused by the sinking of particulate organic matter is a key feature of the biological carbon pump, which helps to store carbon in the deep ocean and reduces atmospheric CO_2 concentration. Depending on the remineralisation depth of organic matter and the residency time of inorganic carbon in the deep ocean (Wilson et al., 2022), a decrease of carbon export caused by climate change might reduce the amount of carbon stored into the deep ocean and increase atmospheric CO_2 concentration, thus forming a positive feedback mechanism. However, the sequestration time of the exported organic carbon strongly vary spatially (Nowicki et al., 2022). In the subtropical North Atlantic Ocean, it is only stored for a few decades, whereas it remains sequestered for several hundred of years in the subpolar North Atlantic Ocean.

The strengthened decrease of carbon export obtained in both regions in this study therefore means that the North Atlantic biological carbon pump might be more affected by climate change than previously anticipated, and on particularly long time scales for the subpolar region. However, because we were not able to reduce diatom NPP projection uncertainties in the region, the spread in carbon export projections remains very large.

Nevertheless, there is no quantitative relationship between carbon export and the efficiency of the biological carbon pump (DeVries et al., 2012). A reduction of the former does not necessarily mean a decrease of the latter. Further work is therefore needed to understand how the decrease in carbon export in the North Atlantic Ocean would affect the biological carbon pump, on both the short and the long term.

5 Conclusion

NPP is a key biogeochemical variable for which we have large uncertainties regarding its future evolution under climate change, particularly in the North Atlantic ocean. The traditional approach to this problem, based on a multi-model mean computed through the "model democracy" approach, fails at providing informative projections for NPP in the region. We therefore developed a new methodology to exploit CMIP6 models diversity, in order to gain new insights in the way NPP will be affected by climate change in the region. Thanks to an innovative regionalisation of the North Atlantic ocean, we were able to identify the processes responsible for the divergence of model projections, and to assess their likelihood to occur. This analysis allowed us to proceed to an informed selection of models in each bioregion, which gave us new estimates of the future evolution of NPP, along with carbon export and plankton biomasses, in the subtropical and subpolar bioregions.

CMIP6 models diversity was essential to conduct such an approach because it allowed us to identify the mechanisms responsible for projection divergence. The models set aside in the different bioregions should therefore not be discarded from CMIP6 ensemble. Nevertheless, it is necessary to recognise that all models are not equally relevant depending on the region and the variable considered, and on the question asked. A direct "model democracy" approach is therefore limited and should only be considered as a first step in an inter-comparison study. It should be completed by more advanced methods, such as informed model selection, observation-based weighting or emergent constraints, and by their combination. Moreover, when CMIP6 models outputs are used to assess the impacts climate change will have on ecosystems or human societies, the relia-

https://doi.org/10.5194/egusphere-2024-1820
Preprint. Discussion started: 3 July 2024

bility of the models used to conduct these studies should be assessed, in order to avoid strong biases stemming from CMIP6 models to affect the results.

Code and data availability. Publicly available datasets were analyzed in this study. This data can be found at: https://esgf.llnl.gov/. The SOM+HAC algorithm used to build the bioregions can be found at : https://github.com/ilarinieminen/SOM-Toolbox

Author contributions. ML, LB and SD conceived the study. SD did the analysis and wrote the paper. REH helped with the construction of the bioregions.

Competing interests. The contact author has declared that none of the authors has any competing interests.

https://doi.org/10.5194/egusphere-2024-1820
Preprint. Discussion started: 3 July 2024

References

Abot, L., Provost, C., and Poli, L.: Recent Convection Decline in the Greenland Sea: Insights From the Mercator Ocean System Over 2008–2020, Journal of Geophysical Research: Oceans, 128, e2022JC019 320, https://doi.org/10.1029/2022JC019320, 2023.

Alexander, K. and Easterbrook, S. M.: The software architecture of climate models: a graphical comparison of CMIP5 and EMICAR5 configurations, Geoscientific Model Development, 8, 1221–1232, https://doi.org/10.5194/gmd-8-1221-2015, publisher: Copernicus GmbH, 2015.

Aumont, O., Ethé, C., Tagliabue, A., Bopp, L., and Gehlen, M.: PISCES-v2: an ocean biogeochemical model for carbon and ecosystem studies, Geoscientific Model Development, 8, 2465–2513, https://doi.org/10.5194/gmd-8-2465-2015, 2015.

Baaklini, G., El Hourany, R., Fakhri, M., Brajard, J., Issa, L., Fifani, G., and Mortier, L.: Surface circulation properties in the eastern Mediterranean emphasized using machine learning methods, Ocean Science, 18, 1491–1505, https://doi.org/10.5194/os-18-1491-2022, publisher: Copernicus GmbH, 2022.

Behrenfeld, M. J. and Falkowski, P. G.: Photosynthetic rates derived from satellite-based chlorophyll concentration, Limnology and Oceanography, 42, 1–20, https://doi.org/10.4319/lo.1997.42.1.0001, 1997.

Benedetti, F., Vogt, M., Elizondo, U. H., Righetti, D., Zimmermann, N. E., and Gruber, N.: Major restructuring of marine plankton assemblages under global warming, Nature Communications, 12, 5226, https://doi.org/10.1038/s41467-021-25385-x, publisher: Nature Publishing Group, 2021.

Bishop, C. H. and Abramowitz, G.: Climate model dependence and the replicate Earth paradigm, Climate Dynamics, 41, 885–900, https://doi.org/10.1007/s00382-012-1610-y, 2013.

Bopp, L., Resplandy, L., Orr, J. C., Doney, S. C., Dunne, J. P., Gehlen, M., Halloran, P., Heinze, C., Ilyina, T., Séférian, R., Tjiputra, J., and Vichi, M.: Multiple stressors of ocean ecosystems in the 21st century: projections with CMIP5 models, Biogeosciences, 10, 6225–6245, https://doi.org/10.5194/bg-10-6225-2013, publisher: Copernicus GmbH, 2013.

Bopp, L., Aumont, O., Kwiatkowski, L., Clerc, C., Dupont, L., Ethé, C., Gorgues, T., Séférian, R., and Tagliabue, A.: Diazotrophy as a key driver of the response of marine net primary productivity to climate change, Biogeosciences, 19, 4267–4285, https://doi.org/10.5194/bg-19-4267-2022, publisher: Copernicus GmbH, 2022.

Boucher, O., Servonnat, J., Albright, A. L., Aumont, O., Balkanski, Y., Bastrikov, V., Bekki, S., Bonnet, R., Bony, S., Bopp, L., Braconnot, P., Brockmann, P., Cadule, P., Caubel, A., Cheruy, F., Codron, F., Cozic, A., Cugnet, D., D'Andrea, F., Davini, P., de Lavergne, C., Denvil, S., Deshayes, J., Devilliers, M., Ducharne, A., Dufresne, J.-L., Dupont, E., Éthé, C., Fairhead, L., Falletti, L., Flavoni, S., Foujols, M.-A., Gardoll, S., Gastineau, G., Ghattas, J., Grandpeix, J.-Y., Guenet, B., Guez, Lionel, E., Guilyardi, E., Guimberteau, M., Hauglustaine, D., Hourdin, F., Idelkadi, A., Joussaume, S., Kageyama, M., Khodri, M., Krinner, G., Lebas, N., Levavasseur, G., Lévy, C., Li, L., Lott, F., Lurton, T., Luyssaert, S., Madec, G., Madeleine, J.-B., Maignan, F., Marchand, M., Marti, O., Mellul, L., Meurdesoif, Y., Mignot, J., Musat, I., Ottlé, C., Peylin, P., Planton, Y., Polcher, J., Rio, C., Rochetin, N., Rousset, C., Sepulchre, P., Sima, A., Swingedouw, D., Thiéblemont, R., Traore, A. K., Vancoppenolle, M., Vial, J., Vialard, J., Viovy, N., and Vuichard, N.: Presentation and Evaluation of the IPSL-CM6A-LR Climate Model, Journal of Advances in Modeling Earth Systems, 12, e2019MS002 010, https://doi.org/10.1029/2019MS002010, _eprint: https://onlinelibrary.wiley.com/doi/pdf/10.1029/2019MS002010, 2020.

Canadell, J. G., Scheel Monteiro, P., Costa, M. H., Cotrim da Cunha, L., Cox, P. M., Eliseev, A. V., Henson, S., Ishii, M., Jaccard, S., Koven, C., Lohila, A., Patra, P. K., Piao, S., Rogelj, J., Syampungani, S., Zaehle, S., and Zickfeld, K.: Global carbon and other biogeochemical cycles and feedbacks, in: Climate Change 2021: The Physical Science Basis. Contribution of Working Group I to the Sixth Assessment

https://doi.org/10.5194/egusphere-2024-1820
Preprint. Discussion started: 3 July 2024

Report of the Intergovernmental Panel on Climate Change, edited by Masson-Delmotte, V., Zhai, P., Pirani, A., Connors, S. L., Péan, C., Berger, S., Caud, N., Chen, Y., Goldfarb, L., Gomis, M. I., Huang, M., Leitzell, K., Lonnoy, E., Matthews, J. B. R., Maycock, T. K., Waterfield, T., Yelekçi, , Yu, R., and Zhou, B., pp. 673–816, Cambridge University Press, Cambridge, United Kingdom and New York, NY, USA, https://doi.org/10.1017/9781009157896.001, 2021.

Christian, J. R., Denman, K. L., Hayashida, H., Holdsworth, A. M., Lee, W. G., Riche, O. G. J., Shao, A. E., Steiner, N., and Swart, N. C.: Ocean biogeochemistry in the Canadian Earth System Model version 5.0.3: CanESM5 and CanESM5-CanOE, Geoscientific Model Development, 15, 4393–4424, https://doi.org/10.5194/gmd-15-4393-2022, publisher: Copernicus GmbH, 2022.

Cox, P. M., Huntingford, C., and Williamson, M. S.: Emergent constraint on equilibrium climate sensitivity from global temperature variability, Nature, 553, 319–322, https://doi.org/10.1038/nature25450, publisher: Nature Publishing Group, 2018.

Derouiche, S., Mallet, C., Hannachi, A., and Bargaoui, Z.: Characterisation of rainfall events in northern Tunisia using self-organising maps, Journal of Hydrology: Regional Studies, 42, 101 159, https://doi.org/10.1016/j.ejrh.2022.101159, 2022.

DeVries, T., Primeau, F., and Deutsch, C.: The sequestration efficiency of the biological pump, Geophysical Research Letters, 39, https://doi.org/10.1029/2012GL051963, _eprint: https://onlinelibrary.wiley.com/doi/pdf/10.1029/2012GL051963, 2012.

Dilmi, M. D., Mallet, C., Barthes, L., and Chazottes, A.: Data-driven clustering of rain events: microphysics information derived from macro-scale observations, Atmospheric Measurement Techniques, 10, 1557–1574, https://doi.org/10.5194/amt-10-1557-2017, publisher: Copernicus GmbH, 2017.

El Hourany, R., Mejia, C., Faour, G., Crépon, M., and Thiria, S.: Evidencing the Impact of Climate Change on the Phytoplankton Community of the Mediterranean Sea Through a Bioregionalization Approach, Journal of Geophysical Research: Oceans, 126, e2020JC016 808, https://doi.org/10.1029/2020JC016808, _eprint: https://onlinelibrary.wiley.com/doi/pdf/10.1029/2020JC016808, 2021.

Eppley, R. W.: Temperature and phytoplankton growth in the sea, 1972.

Eyring, V., Bony, S., Meehl, G. A., Senior, C. A., Stevens, B., Stouffer, R. J., and Taylor, K. E.: Overview of the Coupled Model Intercomparison Project Phase 6 (CMIP6) experimental design and organization, Geoscientific Model Development, 9, 1937–1958, https://doi.org/10.5194/gmd-9-1937-2016, publisher: Copernicus GmbH, 2016.

Eyring, V., Cox, P. M., Flato, G. M., Gleckler, P. J., Abramowitz, G., Caldwell, P., Collins, W. D., Gier, B. K., Hall, A. D., Hoffman, F. M., Hurtt, G. C., Jahn, A., Jones, C. D., Klein, S. A., Krasting, J. P., Kwiatkowski, L., Lorenz, R., Maloney, E., Meehl, G. A., Pendergrass, A. G., Pincus, R., Ruane, A. C., Russell, J. L., Sanderson, B. M., Santer, B. D., Sherwood, S. C., Simpson, I. R., Stouffer, R. J., and Williamson, M. S.: Taking climate model evaluation to the next level, Nature Climate Change, 9, 102–110, https://doi.org/10.1038/s41558-018-0355-y, number: 2 Publisher: Nature Publishing Group, 2019.

Farikou, O., Sawadogo, S., Niang, A., Diouf, D., Brajard, J., Mejia, C., Dandonneau, Y., Gasc, G., Crepon, M., and Thiria, S.: Inferring the seasonal evolution of phytoplankton groups in the Senegalo-Mauritanian upwelling region from satellite ocean-color spectral measurements, Journal of Geophysical Research: Oceans, 120, 6581–6601, https://doi.org/10.1002/2015JC010738, _eprint: https://onlinelibrary.wiley.com/doi/pdf/10.1002/2015JC010738, 2015.

Fox-Kemper, B., Hewitt, H. T., Xiao, C., Aðalgeirsdóttir, G., Drijfhout, S. S., Edwards, T. L., Golledge, N. R., Hemer, M., Kopp, R. E., Krinner, G., Mix, A., Notz, D., Nowicki, S., Nurhati, I. S., Ruiz, L., Sallée, J.-B., Slangen, A. B. A., and Yu, Y.: Ocean, cryosphere, and sea level change, in: Climate Change 2021: The Physical Science Basis. Contribution of Working Group I to the Sixth Assessment Report of the Intergovernmental Panel on Climate Change, edited by Masson-Delmotte, V., Zhai, P., Pirani, A., Connors, S. L., Péan, C., Berger, S., Caud, N., Chen, Y., Goldfarb, L., Gomis, M. I., Huang, M., Leitzell, K., Lonnoy, E., Matthews, J. B. R., Maycock, T. K., Waterfield,

https://doi.org/10.5194/egusphere-2024-1820
Preprint. Discussion started: 3 July 2024

T., Yelekçi, , Yu, R., and Zhou, B., pp. 1211–1362, Cambridge University Press, Cambridge, United Kingdom and New York, NY, USA, https://doi.org/10.1017/9781009157896.001, 2021.

Frieler, K.: Scenario Set-up and the new CMIP6-based climaterelated forcings provided within the third round of the InterSectoral Model Intercomparison Project (ISIMIP3b, group I and II), Geosci. Model Dev., submitted, 2024.

Fu, W., Randerson, J. T., and Moore, J. K.: Climate change impacts on net primary production (NPP) and export production (EP) regulated by increasing stratification and phytoplankton community structure in the CMIP5 models, Biogeosciences, 13, 5151–5170, https://doi.org/10.5194/bg-13-5151-2016, publisher: Copernicus GmbH, 2016.

Garcia, H. E., Weathers, K. W., Paver, C. R., Smolyar, I., Boyer, T. P., Locarnini, R. A., Zweng, M. M., Mishonov, A. V., Baranova, O. K., Seidov, D., and Reagan, J. R.: World Ocean Atlas 2018, Volume 4: Dissolved Inorganic Nutrients (phosphate, nitrate and nitrate+nitrite, silicate), A. Mishonov Technical Ed.; NOAA Atlas NESDIS, 84, 35pp, https://www.ncei.noaa.gov/sites/default/files/2020-04/woa18_vol4.pdf, 2018.

Guèye, A. K., Janicot, S., Niang, A., Sawadogo, S., Sultan, B., Diongue-Niang, A., and Thiria, S.: Weather regimes over Senegal during the summer monsoon season using self-organizing maps and hierarchical ascendant classification. Part I: synoptic time scale, Climate Dynamics, 36, 1–18, https://doi.org/10.1007/s00382-010-0782-6, 2011.

Hilborn, A. and Devred, E.: Delineation of Eastern Beaufort Sea Sub-regions Using Self-Organizing Maps Applied to 17 Years of MODIS-Aqua Data, Frontiers in Marine Science, 9, https://www.frontiersin.org/articles/10.3389/fmars.2022.912865, 2022.

Hofmann Elizondo, U., Righetti, D., Benedetti, F., and Vogt, M.: Biome partitioning of the global ocean based on phytoplankton biogeography, Progress in Oceanography, 194, 102 530, https://doi.org/10.1016/j.pocean.2021.102530, 2021.

Hátún, H., Azetsu-Scott, K., Somavilla, R., Rey, F., Johnson, C., Mathis, M., Mikolajewicz, U., Coupel, P., Tremblay, J.-, Hartman, S., Pacariz, S. V., Salter, I., and Ólafsson, J.: The subpolar gyre regulates silicate concentrations in the North Atlantic, Scientific Reports, 7, 14 576, https://doi.org/10.1038/s41598-017-14837-4, 2017.

Ilyina, T., Six, K. D., Segschneider, J., Maier-Reimer, E., Li, H., and Núñez-Riboni, I.: Global ocean biogeochemistry model HAMOCC: Model architecture and performance as component of the MPI-Earth system model in different CMIP5 experimental realizations, Journal of Advances in Modeling Earth Systems, 5, 287–315, https://doi.org/10.1029/2012MS000178, _eprint: https://onlinelibrary.wiley.com/doi/pdf/10.1029/2012MS000178, 2013.

Jouini, M., Béranger, K., Arsouze, T., Beuvier, J., Thiria, S., Crépon, M., and Taupier-Letage, I.: The Sicily Channel surface circulation revisited using a neural clustering analysis of a high-resolution simulation, Journal of Geophysical Research: Oceans, 121, 4545–4567, https://doi.org/10.1002/2015JC011472, _eprint: https://onlinelibrary.wiley.com/doi/pdf/10.1002/2015JC011472, 2016.

Kearney, K. A., Bograd, S. J., Drenkard, E., Gomez, F. A., Haltuch, M., Hermann, A. J., Jacox, M. G., Kaplan, I. C., Koenigstein, S., Luo, J. Y., Masi, M., Muhling, B., Pozo Buil, M., and Woodworth-Jefcoats, P. A.: Using Global-Scale Earth System Models for Regional Fisheries Applications, Frontiers in Marine Science, 8, https://www.frontiersin.org/articles/10.3389/fmars.2021.622206, 2021.

Kléparski, L., Beaugrand, G., Edwards, M., and Ostle, C.: Phytoplankton life strategies, phenological shifts and climate change in the North Atlantic Ocean from 1850 to 2100, Global Change Biology, 29, 3833–3849, https://doi.org/10.1111/gcb.16709, 2023.

Knutti, R.: The end of model democracy?, Climatic Change, 102, 395–404, https://doi.org/10.1007/s10584-010-9800-2, 2010.

Knutti, R., Sedláček, J., Sanderson, B. M., Lorenz, R., Fischer, E. M., and Eyring, V.: A climate model projection weighting scheme accounting for performance and interdependence, Geophysical Research Letters, 44, 1909–1918, https://doi.org/10.1002/2016GL072012, _eprint: https://onlinelibrary.wiley.com/doi/pdf/10.1002/2016GL072012, 2017.

Kohonen, T.: Essentials of the self-organizing map, Neural Networks, 37, 52–65, https://doi.org/10.1016/j.neunet.2012.09.018, 2013.

https://doi.org/10.5194/egusphere-2024-1820
Preprint. Discussion started: 3 July 2024

Kwiatkowski, L., Bopp, L., Aumont, O., Ciais, P., Cox, P. M., Laufkötter, C., Li, Y., and Séférian, R.: Emergent constraints on projections of declining primary production in the tropical oceans, Nature Climate Change, 7, 355–358, https://doi.org/10.1038/nclimate3265, publisher: Nature Publishing Group, 2017.

Kwiatkowski, L., Torres, O., Bopp, L., Aumont, O., Chamberlain, M., Christian, J. R., Dunne, J. P., Gehlen, M., Ilyina, T., John, J. G., Lenton, A., Li, H., Lovenduski, N. S., Orr, J. C., Palmieri, J., Santana-Falcón, Y., Schwinger, J., Séférian, R., Stock, C. A., Tagliabue, A., Takano, Y., Tjiputra, J., Toyama, K., Tsujino, H., Watanabe, M., Yamamoto, A., Yool, A., and Ziehn, T.: Twenty-first century ocean warming, acidification, deoxygenation, and upper-ocean nutrient and primary production decline from CMIP6 model projections, Biogeosciences, 17, 3439–3470, https://doi.org/10.5194/bg-17-3439-2020, publisher: Copernicus GmbH, 2020.

Laufkötter, C., Vogt, M., Gruber, N., Aita-Noguchi, M., Aumont, O., Bopp, L., Buitenhuis, E., Doney, S. C., Dunne, J., Hashioka, T., Hauck, J., Hirata, T., John, J., Le Quéré, C., Lima, I. D., Nakano, H., Seferian, R., Totterdell, I., Vichi, M., and Völker, C.: Drivers and uncertainties of future global marine primary production in marine ecosystem models, Biogeosciences, 12, 6955–6984, https://doi.org/10.5194/bg-12-6955-2015, publisher: Copernicus GmbH, 2015.

Li, G., Cheng, L., Zhu, J., Trenberth, K. E., Mann, M. E., and Abraham, J. P.: Increasing ocean stratification over the past half-century, Nature Climate Change, 10, 1116–1123, https://doi.org/10.1038/s41558-020-00918-2, publisher: Nature Publishing Group, 2020.

Longhurst, A. R.: Chapter 1 - Toward an ecological geography of the sea, in: Ecological Geography of the Sea (Second Edition), edited by Longhurst, A. R., pp. 1–17, Academic Press, Burlington, ISBN 978-0-12-455521-1, https://doi.org/10.1016/B978-012455521-1/50002-4, 2007.

Masson, D. and Knutti, R.: Climate model genealogy: CLIMATE MODEL GENEALOGY, Geophysical Research Letters, 38, n/a–n/a, https://doi.org/10.1029/2011GL046864, 2011.

Mauritsen, T., Bader, J., Becker, T., Behrens, J., Bittner, M., Brokopf, R., Brovkin, V., Claussen, M., Crueger, T., Esch, M., Fast, I., Fiedler, S., Fläschner, D., Gayler, V., Giorgetta, M., Goll, D. S., Haak, H., Hagemann, S., Hedemann, C., Hohenegger, C., Ilyina, T., Jahns, T., Jimenéz-de-la Cuesta, D., Jungclaus, J., Kleinen, T., Kloster, S., Kracher, D., Kinne, S., Kleberg, D., Lasslop, G., Kornblueh, L., Marotzke, J., Matei, D., Meraner, K., Mikolajewicz, U., Modali, K., Möbis, B., Müller, W. A., Nabel, J. E. M. S., Nam, C. C. W., Notz, D., Nyawira, S.-S., Paulsen, H., Peters, K., Pincus, R., Pohlmann, H., Pongratz, J., Popp, M., Raddatz, T. J., Rast, S., Redler, R., Reick, C. H., Rohrschneider, T., Schemann, V., Schmidt, H., Schnur, R., Schulzweida, U., Six, K. D., Stein, L., Stemmler, I., Stevens, B., von Storch, J.-S., Tian, F., Voigt, A., Vrese, P., Wieners, K.-H., Wilkenskjeld, S., Winkler, A., and Roeckner, E.: Developments in the MPI-M Earth System Model version 1.2 (MPI-ESM1.2) and Its Response to Increasing CO2, Journal of Advances in Modeling Earth Systems, 11, 998–1038, https://doi.org/10.1029/2018MS001400, _eprint: https://onlinelibrary.wiley.com/doi/pdf/10.1029/2018MS001400, 2019.

Moore, J. K., Doney, S. C., Kleypas, J. A., Glover, D. M., and Fung, I. Y.: An intermediate complexity marine ecosystem model for the global domain, Deep Sea Research Part II: Topical Studies in Oceanography, 49, 403–462, https://doi.org/10.1016/S0967-0645(01)00108-4, 2001.

Nowicki, M., DeVries, T., and Siegel, D. A.: Quantifying the Carbon Export and Sequestration Pathways of the Ocean's Biological Carbon Pump, Global Biogeochemical Cycles, 36, e2021GB007 083, https://doi.org/10.1029/2021GB007083, _eprint: https://onlinelibrary.wiley.com/doi/pdf/10.1029/2021GB007083, 2022.

Oke, P. R., Griffin, D. A., Schiller, A., Matear, R. J., Fiedler, R., Mansbridge, J., Lenton, A., Cahill, M., Chamberlain, M. A., and Ridgway, K.: Evaluation of a near-global eddy-resolving ocean model, Geoscientific Model Development, 6, 591–615, https://doi.org/10.5194/gmd-6-591-2013, publisher: Copernicus GmbH, 2013.

https://doi.org/10.5194/egusphere-2024-1820
Preprint. Discussion started: 3 July 2024

O'Neill, B. C., Tebaldi, C., van Vuuren, D. P., Eyring, V., Friedlingstein, P., Hurtt, G., Knutti, R., Kriegler, E., Lamarque, J.-F., Lowe, J., Meehl, G. A., Moss, R., Riahi, K., and Sanderson, B. M.: The Scenario Model Intercomparison Project (ScenarioMIP) for CMIP6, Geoscientific Model Development, 9, 3461–3482, https://doi.org/10.5194/gmd-9-3461-2016, publisher: Copernicus GmbH, 2016.

O'Gorman, P. A.: Sensitivity of tropical precipitation extremes to climate change, Nature Geoscience, 5, 697–700, https://doi.org/10.1038/ngeo1568, publisher: Nature Publishing Group, 2012.

O'Neill, B. C., Kriegler, E., Riahi, K., Ebi, K. L., Hallegatte, S., Carter, T. R., Mathur, R., and van Vuuren, D. P.: A new scenario framework for climate change research: the concept of shared socioeconomic pathways, Climatic Change, 122, 387–400, https://doi.org/10.1007/s10584-013-0905-2, company: Springer Distributor: Springer Institution: Springer Label: Springer Number: 3 Publisher: Springer Netherlands, 2014.

Palter, J. B. and Lozier, M. S.: On the source of Gulf Stream nutrients, Journal of Geophysical Research: Oceans, 113, https://doi.org/10.1029/2007JC004611, _eprint: https://onlinelibrary.wiley.com/doi/pdf/10.1029/2007JC004611, 2008.

Paulsen, H., Ilyina, T., Six, K. D., and Stemmler, I.: Incorporating a prognostic representation of marine nitrogen fixers into the global ocean biogeochemical model HAMOCC, Journal of Advances in Modeling Earth Systems, 9, 438–464, https://doi.org/10.1002/2016MS000737, _eprint: https://onlinelibrary.wiley.com/doi/pdf/10.1002/2016MS000737, 2017.

Qu, X. and Hall, A.: On the persistent spread in snow-albedo feedback, Climate Dynamics, 42, 69–81, https://doi.org/10.1007/s00382-013-1774-0, 2014.

Rohr, T., Richardson, A. J., Lenton, A., Chamberlain, M. A., and Shadwick, E. H.: Zooplankton grazing is the largest source of uncertainty for marine carbon cycling in CMIP6 models, Communications Earth & Environment, 4, 1–22, https://doi.org/10.1038/s43247-023-00871-w, number: 1 Publisher: Nature Publishing Group, 2023.

Räisänen, J., Ruokolainen, L., and Ylhäisi, J.: Weighting of model results for improving best estimates of climate change, Climate Dynamics, 35, 407–422, https://doi.org/10.1007/s00382-009-0659-8, aDS Bibcode: 2010ClDy...35..407R, 2010.

Sanderson, B. M., Knutti, R., and Caldwell, P.: Addressing Interdependency in a Multimodel Ensemble by Interpolation of Model Properties, Journal of Climate, 28, 5150–5170, https://doi.org/10.1175/JCLI-D-14-00361.1, publisher: American Meteorological Society Section: Journal of Climate, 2015.

Sanderson, B. M., Wehner, M., and Knutti, R.: Skill and independence weighting for multi-model assessments, Geoscientific Model Development, 10, 2379–2395, https://doi.org/10.5194/gmd-10-2379-2017, publisher: Copernicus GmbH, 2017.

Sanderson, B. M., Pendergrass, A. G., Koven, C. D., Brient, F., Booth, B. B. B., Fisher, R. A., and Knutti, R.: The potential for structural errors in emergent constraints, Earth System Dynamics, 12, 899–918, https://doi.org/10.5194/esd-12-899-2021, 2021.

Sauterey, B., Gland, G. L., Cermeño, P., Aumont, O., Lévy, M., and Vallina, S. M.: Phytoplankton adaptive resilience to climate change collapses in case of extreme events – A modeling study, Ecological Modelling, 483, 110437, https://doi.org/10.1016/j.ecolmodel.2023.110437, 2023.

Sellar, A. A., Jones, C. G., Mulcahy, J. P., Tang, Y., Yool, A., Wiltshire, A., O'Connor, F. M., Stringer, M., Hill, R., Palmieri, J., Woodward, S., de Mora, L., Kuhlbrodt, T., Rumbold, S. T., Kelley, D. I., Ellis, R., Johnson, C. E., Walton, J., Abraham, N. L., Andrews, M. B., Andrews, T., Archibald, A. T., Berthou, S., Burke, E., Blockley, E., Carslaw, K., Dalvi, M., Edwards, J., Folberth, G. A., Gedney, N., Griffiths, P. T., Harper, A. B., Hendry, M. A., Hewitt, A. J., Johnson, B., Jones, A., Jones, C. D., Keeble, J., Liddicoat, S., Morgenstern, O., Parker, R. J., Predoi, V., Robertson, E., Siahaan, A., Smith, R. S., Swaminathan, R., Woodhouse, M. T., Zeng, G., and Zerroukat, M.: UKESM1: Description and Evaluation of the U.K. Earth System Model, Journal of Advances in Modeling Earth Systems, 11, 4513–4558, https://doi.org/10.1029/2019MS001739, _eprint: https://onlinelibrary.wiley.com/doi/pdf/10.1029/2019MS001739, 2019.

https://doi.org/10.5194/egusphere-2024-1820
Preprint. Discussion started: 3 July 2024

Sieracki, M. E., Verity, P. G., and Stoecker, D. K.: Plankton community response to sequential silicate and nitrate depletion during the 1989 North Atlantic spring bloom, Deep Sea Research Part II: Topical Studies in Oceanography, 40, 213–225, https://doi.org/10.1016/0967-0645(93)90014-E, 1993.

Swart, N. C., Cole, J. N. S., Kharin, V. V., Lazare, M., Scinocca, J. F., Gillett, N. P., Anstey, J., Arora, V., Christian, J. R., Hanna, S., Jiao, Y., Lee, W. G., Majaess, F., Saenko, O. A., Seiler, C., Seinen, C., Shao, A., Sigmond, M., Solheim, L., von Salzen, K., Yang, D., and Winter, B.: The Canadian Earth System Model version 5 (CanESM5.0.3), Geoscientific Model Development, 12, 4823–4873, https://doi.org/10.5194/gmd-12-4823-2019, publisher: Copernicus GmbH, 2019.

Tagliabue, A., Kwiatkowski, L., Bopp, L., Butenschön, M., Cheung, W., Lengaigne, M., and Vialard, J.: Persistent Uncertainties in Ocean Net Primary Production Climate Change Projections at Regional Scales Raise Challenges for Assessing Impacts on Ecosystem Services, Frontiers in Climate, 3, 738 224, https://doi.org/10.3389/fclim.2021.738224, 2021.

Tittensor, D. P., Novaglio, C., Harrison, C. S., Heneghan, R. F., Barrier, N., Bianchi, D., Bopp, L., Bryndum-Buchholz, A., Britten, G. L., Büchner, M., Cheung, W. W. L., Christensen, V., Coll, M., Dunne, J. P., Eddy, T. D., Everett, J. D., Fernandes-Salvador, J. A., Fulton, E. A., Galbraith, E. D., Gascuel, D., Guiet, J., John, J. G., Link, J. S., Lotze, H. K., Maury, O., Ortega-Cisneros, K., Palacios-Abrantes, J., Petrik, C. M., du Pontavice, H., Rault, J., Richardson, A. J., Shannon, L., Shin, Y.-J., Steenbeek, J., Stock, C. A., and Blanchard, J. L.: Next-generation ensemble projections reveal higher climate risks for marine ecosystems, Nature Climate Change, 11, 973–981, https://doi.org/10.1038/s41558-021-01173-9, publisher: Nature Publishing Group, 2021.

Vancoppenolle, M., Bopp, L., Madec, G., Dunne, J., Ilyina, T., Halloran, P. R., and Steiner, N.: Future Arctic Ocean primary productivity from CMIP5 simulations: Uncertain outcome, but consistent mechanisms: FUTURE ARCTIC OCEAN PRIMARY PRODUCTIVITY, Global Biogeochemical Cycles, 27, 605–619, https://doi.org/10.1002/gbc.20055, 2013.

Vatanen, T., Osmala, M., Raiko, T., Lagus, K., Sysi-Aho, M., Orešič, M., Honkela, T., and Lähdesmäki, H.: Self-organization and missing values in SOM and GTM, Neurocomputing, 147, 60–70, https://doi.org/10.1016/j.neucom.2014.02.061, 2015.

Wang, W.-L., Moore, J. K., Martiny, A. C., and Primeau, F. W.: Convergent estimates of marine nitrogen fixation, Nature, 566, 205–211, https://doi.org/10.1038/s41586-019-0911-2, number: 7743 Publisher: Nature Publishing Group, 2019.

Weijer, W., Cheng, W., Garuba, O. A., Hu, A., and Nadiga, B. T.: CMIP6 Models Predict Significant 21st Century Decline of the Atlantic Meridional Overturning Circulation, Geophysical Research Letters, 47, e2019GL086 075, https://doi.org/10.1029/2019GL086075, 2020.

Westberry, T., Behrenfeld, M. J., Siegel, D. A., and Boss, E.: Carbon-based primary productivity modeling with vertically resolved photoacclimation, Global Biogeochemical Cycles, 22, 2007GB003 078, https://doi.org/10.1029/2007GB003078, 2008.

Whitt, D. B.: On the Role of the Gulf Stream in the Changing Atlantic Nutrient Circulation During the 21st Century, in: Geophysical Monograph Series, edited by Nagai, T., Saito, H., Suzuki, K., and Takahashi, M., pp. 51–82, Wiley, 1 edn., ISBN 978-1-119-42834-3 978-1-119-42842-8, https://doi.org/10.1002/9781119428428.ch4, 2019.

Williams, R. G., Roussenov, V., and Follows, M. J.: Nutrient streams and their induction into the mixed layer: NUTRIENT STREAMS AND INDUCTION, Global Biogeochemical Cycles, 20, n/a–n/a, https://doi.org/10.1029/2005GB002586, 2006.

Williams, R. G., McDonagh, E., Roussenov, V. M., Torres-Valdes, S., King, B., Sanders, R., and Hansell, D. A.: Nutrient streams in the North Atlantic: Advective pathways of inorganic and dissolved organic nutrients, Global Biogeochemical Cycles, 25, https://doi.org/10.1029/2010GB003853, _eprint: https://onlinelibrary.wiley.com/doi/pdf/10.1029/2010GB003853, 2011.

Wilson, J. D., Andrews, O., Katavouta, A., de Melo Viríssimo, F., Death, R. M., Adloff, M., Baker, C. A., Blackledge, B., Goldsworth, F. W., Kennedy-Asser, A. T., Liu, Q., Sieradzan, K. R., Vosper, E., and Ying, R.: The biological carbon pump in CMIP6 models: 21st century

https://doi.org/10.5194/egusphere-2024-1820
Preprint. Discussion started: 3 July 2024

trends and uncertainties, Proceedings of the National Academy of Sciences, 119, e2204369 119, https://doi.org/10.1073/pnas.2204369119, publisher: Proceedings of the National Academy of Sciences, 2022.

Yahi, H., Marticorena, B., Thiria, S., Chatenet, B., Schmechtig, C., Rajot, J. L., and Crepon, M.: Statistical relationship between surface PM10 concentration and aerosol optical depth over the Sahel as a function of weather type, using neural network methodology, Journal of Geophysical Research: Atmospheres, 118, 13,265–13,281, https://doi.org/10.1002/2013JD019465, _eprint: https://onlinelibrary.wiley.com/doi/pdf/10.1002/2013JD019465, 2013.

Yool, A., Popova, E. E., and Anderson, T. R.: MEDUSA-2.0: an intermediate complexity biogeochemical model of the marine carbon cycle for climate change and ocean acidification studies, Geoscientific Model Development, 6, 1767–1811, https://doi.org/10.5194/gmd-6-1767-2013, publisher: Copernicus GmbH, 2013.

Zahariev, K., Christian, J. R., and Denman, K. L.: Preindustrial, historical, and fertilization simulations using a global ocean carbon model with new parameterizations of iron limitation, calcification, and N2 fixation, Progress in Oceanography, 77, 56–82, https://doi.org/10.1016/j.pocean.2008.01.007, 2008.

Ziehn, T., Chamberlain, M. A., Law, R. M., Lenton, A., Bodman, R. W., Dix, M., Stevens, L., Wang, Y.-P., and Srbinovsky, J.: The Australian Earth System Model: ACCESS-ESM1.5, Journal of Southern Hemisphere Earth Systems Science, 70, 193–214, https://doi.org/10.1071/ES19035, publisher: CSIRO PUBLISHING, 2020.

https://doi.org/10.5194/egusphere-2024-1820
Preprint. Discussion started: 3 July 2024

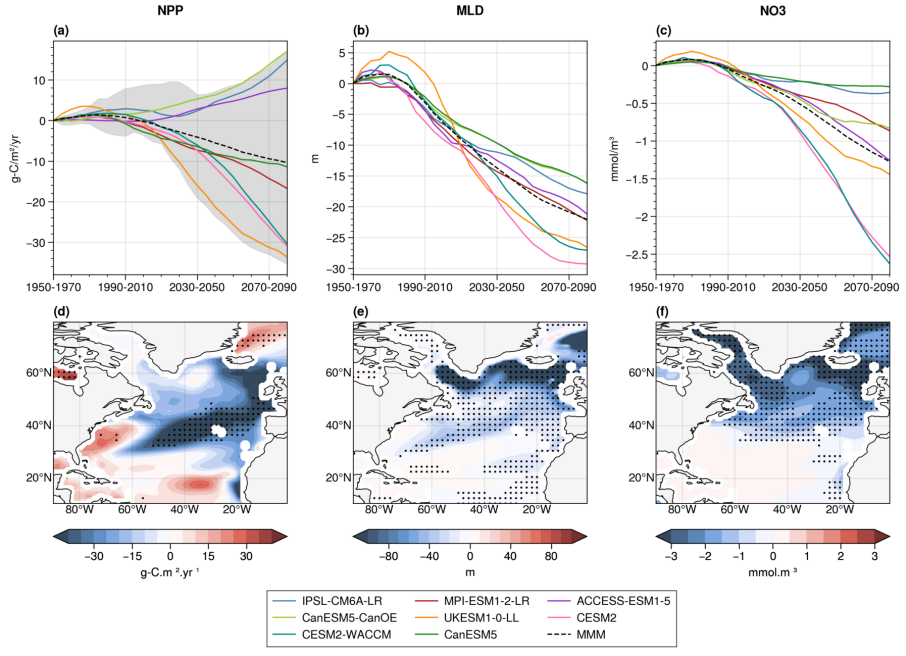

Figure 1. Projections of NPP (A), mixed layer depth (B) and surface NO3 concentrations (C) in the eight CMIP6 models over the whole North Atlantic Ocean. The dotted black lines are the multi-model means (MMM) and the shaded area in the NPP panel corresponds to the range of projections with the first member of the 16 models used in Tagliabue et al. (2021). Maps of the evolution of NPP (D), mixed layer depth (E) and surface NO3 concentrations (F) between 1950-1970 and 2080-2100. Stippling designates areas of projection robustness, defined as 80 % model sign agreement.

https://doi.org/10.5194/egusphere-2024-1820
Preprint. Discussion started: 3 July 2024

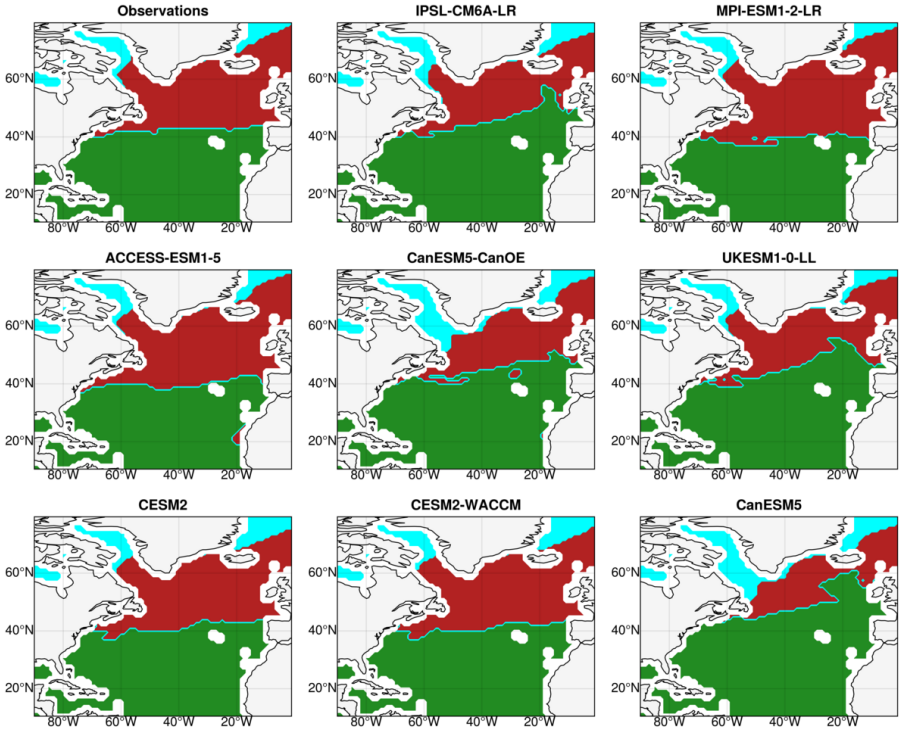

Figure 2. Bioregions built with the SOM+HAC procedure from the historical seasonal cycles of chlorophyll-a concentrations, nitrate concentrations, SST, MLD and sea ice concentration, and their reproduction in CMIP6 models for the period 2000-2020. The subtropical region is in green, the subpolar one in red and the polar region is in cyan.

https://doi.org/10.5194/egusphere-2024-1820
Preprint. Discussion started: 3 July 2024

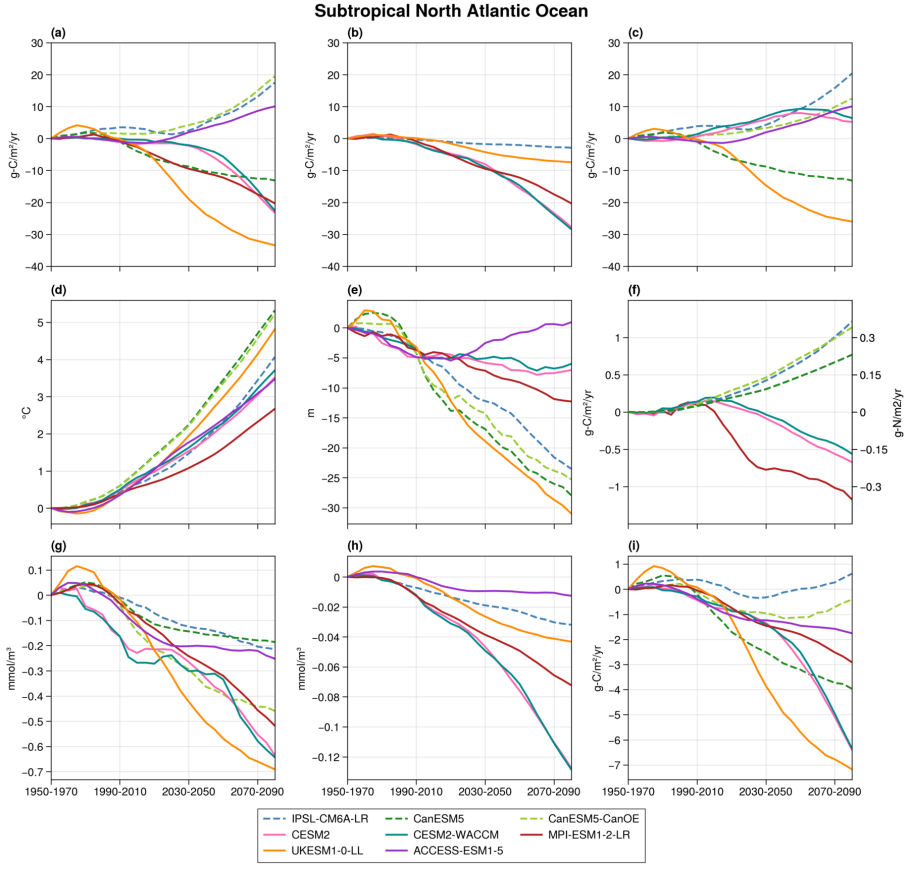

Figure 3. Projections over the subtropical bioregion of total NPP (a), diatom NPP (b), small phytoplankton NPP (c), SST (d), MLD (e), diazotrophy (f), nitrate concentrations (g), phosphate concentrations (h) and carbon export at 100 m depth (i). The average value over 1950-1970 is taken as the reference. The dotted lines correspond to the three models with a parametrized N2 fixation. On panel F, these three models refer to the right-hand axis.

https://doi.org/10.5194/egusphere-2024-1820
Preprint. Discussion started: 3 July 2024

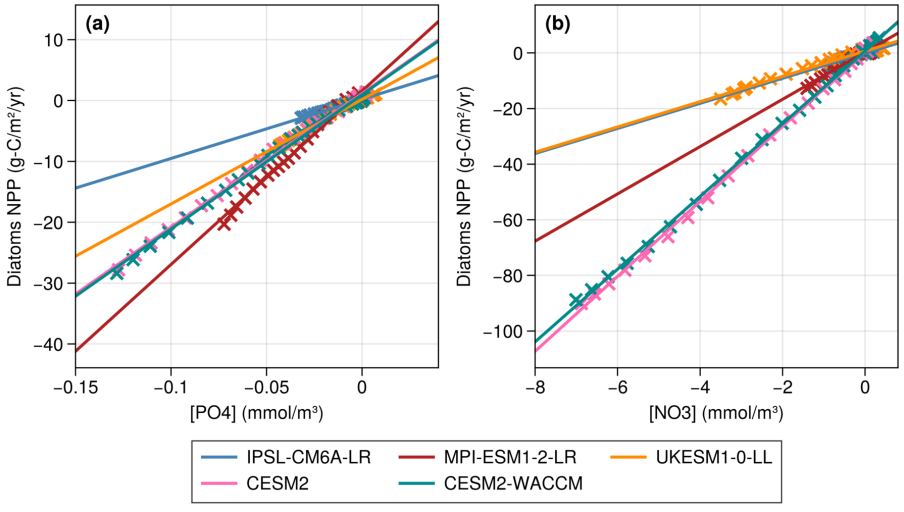

Figure 4. Correlations between the evolutions of diatom NPP and surface maximum annual macro-nutrient concentrations between 1950-1970 and 2080-2100 in the subtropical region (A) and in the subpolar one (B).

https://doi.org/10.5194/egusphere-2024-1820
Preprint. Discussion started: 3 July 2024

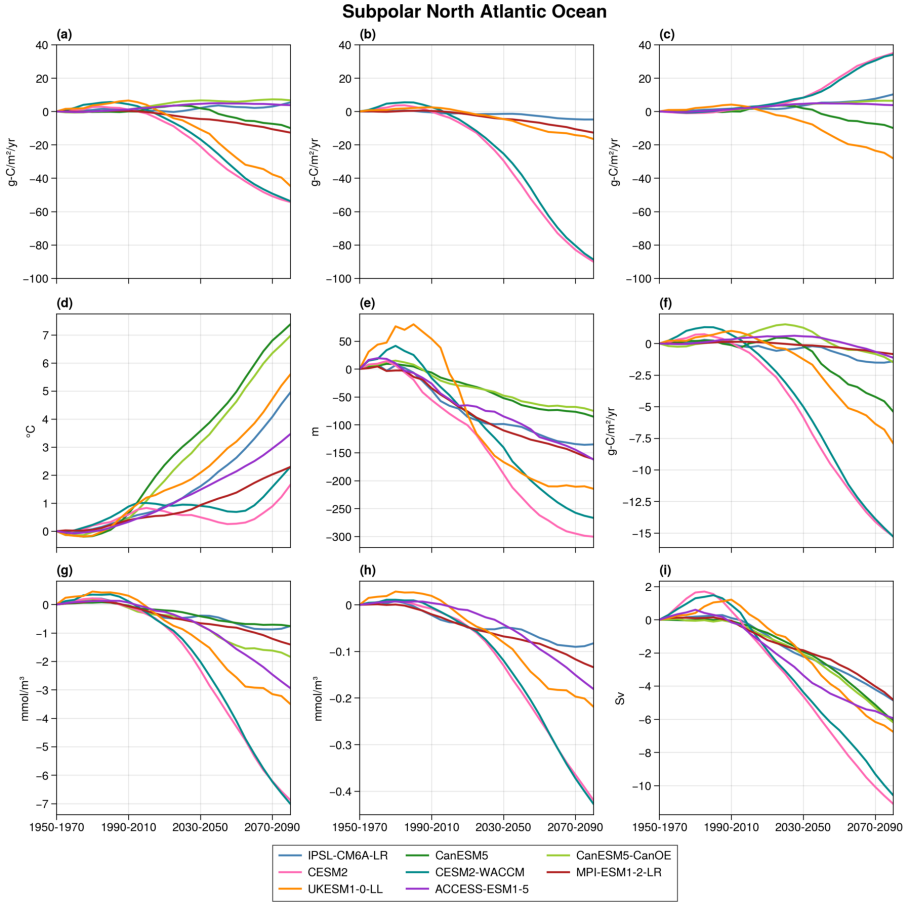

Figure 5. Projections over the subpolar bioregion of total NPP (a), diatom NPP (b), small phytoplankton NPP (c), SST (d), MLD (e), carbon export (f), nitrate concentrations (g), phosphate concentrations (h) and AMOC (i). The average value over 1950-1970 is taken as the reference.

https://doi.org/10.5194/egusphere-2024-1820
Preprint. Discussion started: 3 July 2024

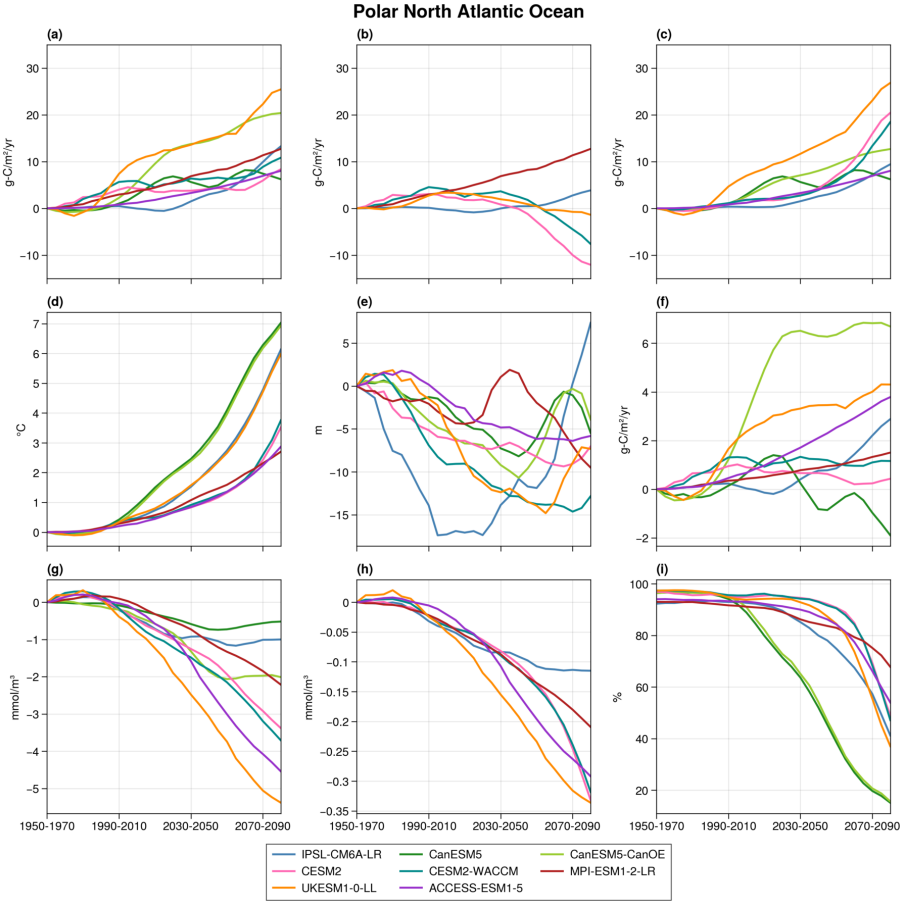

Figure 6. Projections over the polar bioregion of total NPP (a), diatom NPP (b), small phytoplankton NPP (c), SST (d), MLD (e), carbon export (f), nitrate concentrations (g), phosphate concentrations (h) and sea ice concentration (i). The average value over 1950-1970 is taken as the reference.

https://doi.org/10.5194/egusphere-2024-1820
Preprint. Discussion started: 3 July 2024

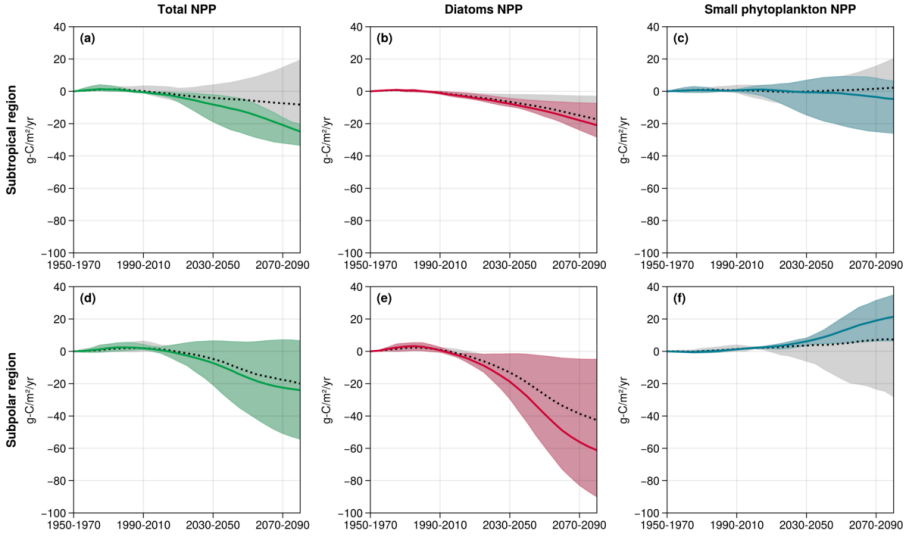

Figure 7. New estimates of total NPP (panels A and D), diatom NPP (B and E) and small phytoplankton's NPP (C and F) projections with the selected CMIP6 models in the subtropical (top row) and subpolar (bottom row) regions. The grey shaded areas and the dotted black lines respectively correspond to the projection inter-model spreads with all models and the associated multi-model means. The coloured shaded areas and the plain lines correspond to the new inter-model spreads and multi-model means with the selected models.

https://doi.org/10.5194/egusphere-2024-1820
Preprint. Discussion started: 3 July 2024

Model	Ocean and sea ice	Marine biogeochemistry	Phytoplankton groups	Nbr of members	Reference
ACCESS-ESM1-5	MOM5, CICE4	WOMBAT	Phytoplankton	10	Ziehn et al. (2020); Oke et al. (2013)
CESM2	POP2-CICE5	MARBL-BEC	Picophytoplankton Diatoms Diazotrophs	3	Moore et al. (2001)
CESM2-WACCM	POP2-CICE5	MARBL-BEC	Picophytoplankton Diatoms Diazotrophs	3	Moore et al. (2001)
CanESM5	NEMOv3.4.1-LIM2	CMOC	Phytoplankton Diazotrophs (param.)	5	Swart et al. (2019); Christian et al. (2022); Zahariev et al. (2008)
CanESM5-CanOE	NEMOv3.4.1-LIM2	CanOE	Nanophytoplankton Microphytoplankton Diazotrophs (param.)	3	Swart et al. (2019); Christian et al. (2022)
IPSL-CM6A-LR	NEMOv3.6-LIM3	PISCESv2	Nanophytoplankton Diatoms Diazotrophs (param.)	7	Boucher et al. (2020); Aumont et al. (2015)
MPI-ESM1-2-LR	MPIOM1	HAMOCC6	Diatoms Diazotrophs	10	Mauritsen et al. (2019); Paulsen et al. (2017)
UKESM1-0-LL	NEMOv3.6, CICE	MEDUSA-2	Nanophytoplankton Diatoms	5	Sellar et al. (2019); Yool et al. (2013)

Table 1. Characteristics of the 8 CMIP6 models studied. The phytoplankton group "Diatoms (param.)" refers to models with an implicit representation of N2 fixation with a parametrization and without an explicit diazotroph group.

https://doi.org/10.5194/egusphere-2024-1820
Preprint. Discussion started: 3 July 2024

		Total NPP ($g.m^{-2}.yr^{-1}$)	Export C (100m) ($g.m^{-2}.yr^{-1}$)	Phyto biomass ($g\text{-}C/m^3$)	Zoo biomass ($g\text{-}C/m^3$)
North Atlantic Ocean	All models	-10.4 [-33.7 - +17.0]	-3.9 [-8.7 - +0.3]	-0.22 [-0.64 - +0.21]	-0.16 [-0.56 - -0.01]
Subtropical region	All models	-8,2 [-33.4 - +19.5]	-3.5 [-7.2 - +0.6]	-0.16 [-0.63 - +0.24]	-0.17 [-0.59 - -0.01]
	Subset	-24.9 [-33.4 - -20.3]	-5.7 [-7.2 - -2.9]	-0.27 [-0.63 - -0.13]	-0.22 [-0.59 - -0.08]
Subpolar region	All models	-20.0 [-54.3 - +6.6]	-6.1 [-15.3 - -0.8]	-0.48 [-0.86 - +0.07]	-0.17 [-0.6 - +0.0]
	Subset	-24.0 [-54.3 - +6.6]	-8.4 [-15.3 - -1.4]	-0.50 [-0.68 - +0.07]	-0.13 [-0.48 - +0.0]

Table 2. Comparison of the mean projections of total NPP, carbon export at 100m, phytoplankton and zooplankton biomasses between 1950-1970 and 2080-2100 in the subtropical and subpolar regions for all models and for the subsets determined in each region. The values within the brackets correspond to inter-model spread.